ELSEVIER

Marine Geology 161 (1999) 171–190

MARINE GEOLOGY
INTERNATIONAL JOURNAL OF MARINE GEOLOGY, GEOCHEMISTRY AND GEOPHYSICS

www.elsevier.nl/locate/margeo

Variability in Late Cretaceous climate and deep waters: evidence from stable isotopes

Liangquan Li, Gerta Keller *

Department of Geosciences, Princeton University, Princeton, 08544, USA

Received 20 November 1997; accepted 18 June 1999

Abstract

Strong climatic and temperature fluctuations mark the Late Campanian and Maastrichtian as indicated by stable isotope records from the equatorial Pacific (Site 463) and middle and high latitude South Atlantic (Sites 525, 689 and 690). The first major global cooling decreased intermediate water temperatures (IWT) by 5–6°C between 73–70 Ma. At the same time, sea surface temperature (SST) decreased by 4–5°C in middle and high latitudes. Intermediate waters (IW) temporarily warmed by 2°C in low and middle latitudes between 70–68.5 Ma. Global cooling resumed between 68.5–65.5 Ma when IWT decreased by 3–4°C and SST by 5°C in middle latitudes. About 450 ka before the Cretaceous–Tertiary boundary rapid global warming increased IWT and SST by 3–4°C, though SST in the tropics changed little. During the last 200 ka of the Maastrichtian, climate cooled rapidly with IWT and SST decreasing by 2–3°C. During the global cooling at 71–70 Ma and possibly at 67–65.5 Ma, the sources of cold intermediate waters in the equatorial Pacific, Indo-Pacific and South Atlantic were derived from the high latitude North Pacific. In contrast, during the global climate warming between 65.2–65.4 Ma, the middle latitude South Atlantic was closest to the source of IW production and implies that the low latitude Tethys played a major role in global climate change. Climate changes, sea-level fluctuations and associated restricted seaways appear to be the most likely mechanisms for the alternating sources of IW production.

Keywords: Maastrichtian; Stable isotopes; Climate; Deep-water

1. Introduction

One of the most striking features in Earth's climate history is the transition from a very warm middle Cretaceous to a relatively cool late Cretaceous climate (Douglas and Savin, 1973, 1975; Arthur et al., 1985; Barrera et al., 1987; Barrera et al., 1997; Spicer and Corfield, 1992; D'Hondt and Lindinger, 1994; Huber et al., 1995; D'Hondt and Arthur, 1996; Li and Keller, 1998a,c). This cooling trend was accompanied by three third-order global sea-level regressions during the late Campanian and Maastrichtian at about 74.5 Ma, 71–70 Ma and 68–67 Ma, which were estimated to have lowered sea-level by ~50 m, ~70 m and ~100 m respectively (Haq et al., 1987; Li et al., 1999, Li et al., in press). Though the cause for the late Cretaceous cooling and sea-level regressions is still unknown, various authors speculate that they might be related

* Corresponding author. Fax: +1-609-258-1274; E-mail: gkeller@princeton.edu

0025-3227/99/$ - see front matter
PII: S0025-3227(99)00078-X

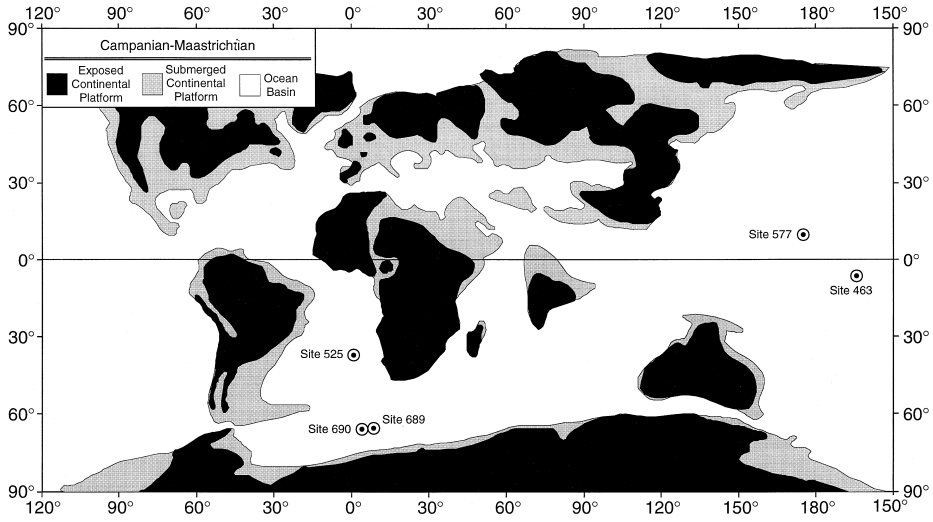

Fig. 1. Locations of DSDP and ODP sites discussed in this report.

to ice build-up in high latitudes (Matthews and Poore, 1980; Barrera, 1994; Abreu et al., 1998), the reversal in thermohaline circulation at 71–70 Ma (Barrera et al., 1997; MacLeod and Huber, 1997), and tectonic barriers to ocean circulation (Frank and Arthur, 1999).

The main objectives of this study are to reconstruct late Campanian and Maastrichtian seawater paleotemperatures, latitudinal and vertical thermal gradients, and surface productivity, and evaluate sources and modes of intermediate water circulation and potential mechanisms for global climate changes. Our database consists of new stable isotope data from DSDP Site 463, and correlation and comparison with published isotope records from southern high latitude ODP Sites 689 and 690 (Barrera and Huber, 1990; Stott and Kennett, 1990), middle latitude South Atlantic DSDP Site 525 (Li and Keller, 1998a,c) and low latitude Pacific DSDP Site 577 (Zachos et al., 1985, 1989). These sections span paleolatitudes 5°S, 36–38°S and 65°S and were deposited at paleodepths ranging from 1000 m to 2100 m (Fig. 1; Table 1).

2. Material and methods

For the late Campanian and Maastrichtian interval from equatorial Pacific DSDP Site 463, monospecific planktic and benthic foraminifers were analyzed at approximately 1.5 m sample spacing (84 samples, cores 7 to 25). Samples were disaggregated in water, washed through a 63 μm sieve and dried in the oven at < 50°C. Surface temperatures were obtained from $\delta^{18}O$ measurements of about 30 adult tests of the surface dweller *Rugoglobigerina rugosa* in the 150–250 μm size fraction. Bottom water temperatures were obtained from about 20 adult tests of the benthic *Nuttalides truempyi* in the 150–250 μm size fraction. Stable isotope analyses were conducted at the stable isotope laboratory of Princeton University using a VG Optima gas source mass spectrometer equipped with a common acid bath. All isotopic ratios are reported in the δ-notation and calibrated to the Pee Dee Belemnite (PDB) standard (Table 2). The precision of replicate measurements is 0.05‰

Table 1
Paleolatitudes and paleodepths for the sites used in this study

Site	Paleo-latitude	Paleodepth	References
DSDP Site 463	~ 5°S	1500 m	Boersma, 1981
DSDP Site 525	36°S	1000–1500 m	Chave, 1984; Moore et al., 1984
DSDP Site 577	10°N	2400 m	Zachos et al., 1985
ODP Site 689	65°S	1000–1500 m	Thomas, 1990
ODP Site 690	65°S	1500–200 m	Thomas, 1990

for $\delta^{18}O$ and 0.03‰ for $\delta^{13}C$. Seawater paleotemperatures were estimated using the $\delta^{18}O$ equation of Erez and Luz (1983). The mean value of seawater $\delta^{18}O$ of -1.0‰ has been applied to estimate paleotemperature in seawaters largely free from the influence of major ice sheets (Shackleton and Kennett, 1975).

2.1. Preservation and diagenesis

The preservation of Maastrichtian foraminiferal species at Site 463 is generally good with little recrystallization of test calcite, though dissolution effects are noted in cores 18–16 and 12–11 (Boersma, 1981; Barrera et al., 1997). Dissolution may change surface water $\delta^{18}O$ values towards cooler temperatures (Paull et al., 1988; Wu and Berger, 1990). In addition, secondary recrystallization of planktic foraminiferal tests after settling on the seafloor may alter planktic $\delta^{18}O$ towards high values.

Though it is always difficult to evaluate the effects of preservation and diagenesis on oxygen isotope values, a number of tests can be done to evaluate recrystallization including SEM investigation of foraminiferal shells and plots of $\delta^{18}O$ vs. Sr/Ca ratios. For the late Campanian–Maastrichtian at Site 463, calcite recrystallization was only observed in two isolated samples in cores 10 and 13 (Boersma, 1981). To evaluate diagenetic effects of the foraminiferal tests, we plotted Sr/Ca ratios vs. $\delta^{18}O$ values in Fig. 2a and b. Generally, diagenetic processes reduce Sr concentrations in calcite because of the similar chemistry of Sr and Ca (Baker et al., 1982; Richter and Liang, 1993). Thus, strong diagenetic effects result in a good correlation between Sr/Ca ratios and $\delta^{18}O$ values due to the loss of Sr. Our data show a low correlation coefficient between the Sr/Ca ratio of *Heterohelix globulosa* and $\delta^{18}O$ values for planktic ($R^2 = 0.12$) and benthic foraminifers ($R^2 = 0.19$), which suggests that there are no major diagenetic effects. However, the point scatter is large and diagenesis could affect some samples and not others. Time series analyses of oxygen isotopes and Sr/Ca ratios provide a better visual assessment of foraminiferal test preservation as shown in Fig. 2c. The trends evident in these time series analyses indicate that although diagenesis may affect individual samples, the longterm trends appear real. Moreover, the longterm trends in the oxygen isotope records mirror those of Sites 525, 690 and 689 which are considered as relatively unaltered by diagenesis (Barrera and Huber, 1990; Stott and Kennett, 1990; Barrera, 1994; Barrera et al., 1997; Li and Keller, 1998a,c).

Vital effects, including different test sizes of a single species may also affect the original stable isotopic signals in foraminifera (Erez and Luz, 1983; Spero, 1992; Spero and Williams, 1988; Spero et al., 1991). However, variations due to test size differences can be minimized by analyzing narrowly constrained size fractions (150–250 μm) as was done for this study. Among different benthic foraminiferal species, disequilibrium factors can be adjusted to obtain paleotemperature estimates. For *Nuttalides truempyi* (Site 463), the disequilibrium adjustment factor is 0.35‰ in $\delta^{18}O$. For *Gavelinella* spp. (Sites 689 and 690), it is 0.30‰ in $\delta^{18}O$ and for *Anomalinoides* spp. (Site 525) it is 0.3‰ in both $\delta^{18}O$ and $\delta^{13}C$ (Shackleton et al., 1984).

3. Biostratigraphy

The planktic foraminiferal biozonation of Site 463 is based on Caron (1985) with the late Maastrichtian refined by Li and Keller (1998a; b) and Li et al. (1999) as illustrated in Fig. 3. Most of the late Maastrichtian (biozones CF1, CF2 and CF3) is missing at Site 463 due to a major hiatus that also spans the Cretaceous–Tertiary (K–T) boundary (missing interval from 67.5 to 64.5 Ma, Figs. 3 and 4). The late Cretaceous interval (67.5–75.5 Ma) below this hiatus is relatively continuous, except for a condensed interval or short hiatus in Zone CF9 (74–73 Ma) as suggested by the low sedimentation rate (8.1 m/Ma, Fig. 4). A relatively continuous record between 73 Ma and 65 Ma is present at Sites 525, 689 and 690.

3.1. Campanian–Maastrichtian boundary

This boundary has not been formally defined. In this study, we follow Gradstein et al. (1994) who proposed the placement of this boundary at 71.6 ± 0.7 Ma (based on linear interpolation between K/Ar

Table 2
Stable isotopic data of mono-specific foraminiferal samples from DSDP Site 463

Core-section	Interval (cm)	Depth (mbsf)	*Nuttalides truempyi*		*Rugoglobigerina rugosa*	
			$\delta^{13}C$ (PDB)	$\delta^{18}O$ (PDB)	$\delta^{13}C$ (PDB)	$\delta^{18}O$ (PDB)
7-3	51–53	47.02	0.81	0.61	2.03	−0.89
7-3	97–99	47.48	1.00	0.73	2.03	−0.82
7-4	48–50	48.49	1.04	0.85	2.11	−0.88
8-1	99–101	54.00	0.72	0.24	2.17	−1.00
8-2	99–101	55.50	0.80	0.45		
8-3	50–53	56.51	0.97	0.52	2.22	−1.12
9-1	100–102	63.51	1.24	0.51	2.26	−1.04
9-3	102–104	66.53	1.28	0.49	2.31	−1.09
10-1	96–98	72.97	1.22	0.33	2.29	−1.04
10-2	99–102	74.51	1.16	0.41	2.14	−1.07
10-3	101–103	76.02	1.15	0.29	2.27	−1.28
10-4	100–102	77.51	1.12	0.37	2.33	−1.08
10-5	97–99	78.98	1.11	0.37	2.17	−1.03
10-6	101–104	80.53	1.07	0.39	2.24	−1.25
11-1	125–127	82.76	1.05	0.64	2.46	−1.17
11-2	122–124	84.25	1.12	0.51	2.33	−1.08
11-3	100–104	85.03	1.16	0.31	2.30	−0.98
11-4	100–102	87.01	1.13	0.49	2.33	−1.21
11-5	45–47	87.96	0.88	0.47	2.47	−1.10
12-1	98–100	91.99	0.94	0.55	2.51	−1.06
12-2	100–102	92.51	0.88	0.53	2.40	−1.08
12-3	98–100	94.99	0.77	0.39	2.31	−1.16
12-4	98–100	96.49	0.80	0.45		
12-5	103–105	98.04	0.91	0.65	2.48	−1.04
12-6	100–102	99.51	0.96	0.48	2.38	−1.20
13-1	103–105	101.54	0.76	0.94	2.66	−1.28
13-2	78–80	102.79	0.72	0.76	2.62	−1.20
13-3	97–99	104.48	0.77	0.78	2.69	−1.13
13-4	100–102	106.02	0.59	0.91	2.64	−1.22
13-5	98–100	107.49	0.84	0.74	2.60	−1.08
13-6	75–77	108.76	0.84	0.90	2.67	−1.08
14-1	98–100	110.99	0.57	0.91	2.51	−1.24
14-2	100–102	112.51	0.59	0.97	2.59	−1.30
14-3	103–105	114.04	0.70	0.85	2.56	−1.17
14-4	100–102	115.51	0.75	0.80	2.68	−1.19
15-1	102–104	120.53	0.32	0.70	2.52	−1.26
15-2	99–103	122.01	0.30	0.60	2.41	−1.27
15-3	96–98	123.47	0.61	0.69	2.27	−1.51
15-4	100–102	125.01	0.80	0.66		
15-5	100–102	126.51	0.45	0.73	2.31	−1.40
16-1	128–130	130.29	0.71	0.62	2.26	−1.16
16-2	124–126	131.75	0.76	0.57	2.48	−1.10
16-3	95–98	132.96	0.66	0.56	2.44	−1.05
16-4	94–96	134.45	0.67	0.56	2.45	−1.13
16-5	53–55	135.54	0.70	0.69	2.44	−1.04
16-6	101–103	137.52	0.63	0.57	2.47	−1.33
17-1	100–102	139.51	1.03	0.01	2.43	−1.09
17-2	95–97	140.96	0.81	0.36	2.44	−1.20
17-3	94–96	142.45	0.78	0.42	2.33	−1.30
17-4	98–100	143.99	0.80	0.28	2.40	−1.21
17-5	98–100	145.49	0.74	0.24	2.45	−1.07

Table 2 (continued)

Core-section	Interval (cm)	Depth (mbsf)	*Nuttalides truempyi*		*Rugoglobigerina rugosa*	
			$\delta^{13}C$ (PDB)	$\delta^{18}O$ (PDB)	$\delta^{13}C$ (PDB)	$\delta^{18}O$ (PDB)
17-6	98–100	146.99	0.53	0.52	2.46	−1.35
18-1	20–22	148.21	0.75	0.11	2.54	−1.36
18-1	98–100	148.99	0.44	0.35	2.27	−1.07
19-1	23–25	157.74	0.90	0.29	2.29	−1.30
19-1	100–102	158.51	0.73	0.19	2.38	−1.10
19-2	97–99	159.98	0.99	0.22	2.35	−1.23
19-3	102–104	161.53	0.93	0.30	2.28	−1.00
19-4	102–104	163.03	0.89	0.33	2.30	−1.11
19-5	102–104	164.53	0.94	0.20	2.15	−1.24
19-6	103–105	166.04	0.87	0.19	2.23	−1.13
20-1	20–22	167.21	1.01	0.01	2.77	−1.44
20-1	100–102	168.01	1.04	0.03	2.98	−1.34
21-1	20–22	176.71	0.74	−0.08	2.80	−1.26
21-1	98–100	177.49	0.87	−0.04	2.68	−1.46
21-2	108–110	179.09	0.77	0.03	2.58	−1.42
21-3	103–105	180.54	0.85	−0.17	2.59	−1.38
21-4	103–105	182.04	0.86	−0.14	2.60	−1.39
21-5	64–66	183.15	0.79	−0.04	2.67	−1.20
21-6	97–99	184.98	0.77	−0.04	2.58	−1.22
22-1	97–99	186.98	0.71	0.05	2.56	−1.22
22-2	105–107	188.56	0.78	0.02	2.55	−1.70
22-3	105–107	190.06	0.68	0.11	2.53	−1.36
22-4	103–105	191.54	0.78	0.20	2.32	−1.56
22-5	46–48	192.47	0.88	0.11	2.32	−1.37
23-1	20–22	195.71	1.07	0.07	2.48	−1.17
23-1	120–122	196.71	0.92	0.23	2.31	−1.08
24-1	20–22	199.71	0.85	−0.14	2.18	−1.09
24-1	101–103	200.52	1.03	0.06	2.31	−1.17
24-2	126–128	202.27	0.97	0.12	2.18	−1.24
24-3	101–103	203.52	0.83	−0.02	2.41	−1.39
25-1	28–30	205.29	0.69	0.10	2.15	−1.01
25-1	98–100	205.99	0.51	0.08		
25-2	86–88	207.37	1.22	0.02	2.17	−1.12

ages of two bentonites at 70.1 ± 0.7 Ma and 73.2 ± 0.7 Ma). This interval corresponds to within the upper *G. aegyptiaca* Zone and near the first appearances of the planktic foraminifera *Rugoglobigerina hexacamerata* and *Planoglobulina carseyae*, which subdivide this zone (CF8) into two Subzones CF8a and CF8b (Fig. 3). We tentatively use the planktic foraminiferal datum of *R. hexacamerata* (at 71 Ma at DSDP Site 525) to mark the Campanian–Maastrichtian boundary in this study.

3.2. Early–late Maastrichtian

Though this boundary has not yet been formally defined (Odin, 1996 p. 115), planktic foraminiferal workers have generally placed it at the first appearance (FA) of *G. gansseri* (Robaszynski et al., 1983-84; Caron, 1985; Li and Keller, 1998a,b), or at the FA of *A. mayaroensis* or *R. fructicosa* (Boersma, 1981; Nederbragt, 1991). However, *A. mayaroensis* is a poor biostratigraphic marker because this species, which is known to be diachronous (Keller, 1989; Huber, 1990; Pardo et al., 1996), appears much earlier in high latitudes and is rare or absent in neritic environments. Gradstein et al. (1994 p. 110) proposed that the early-late Maastrichtian boundary be placed at 69.5 Ma within the upper part of C31R. This interval corresponds to the first appearance of *Rosita contusa* at DSDP Site 525 which marks the

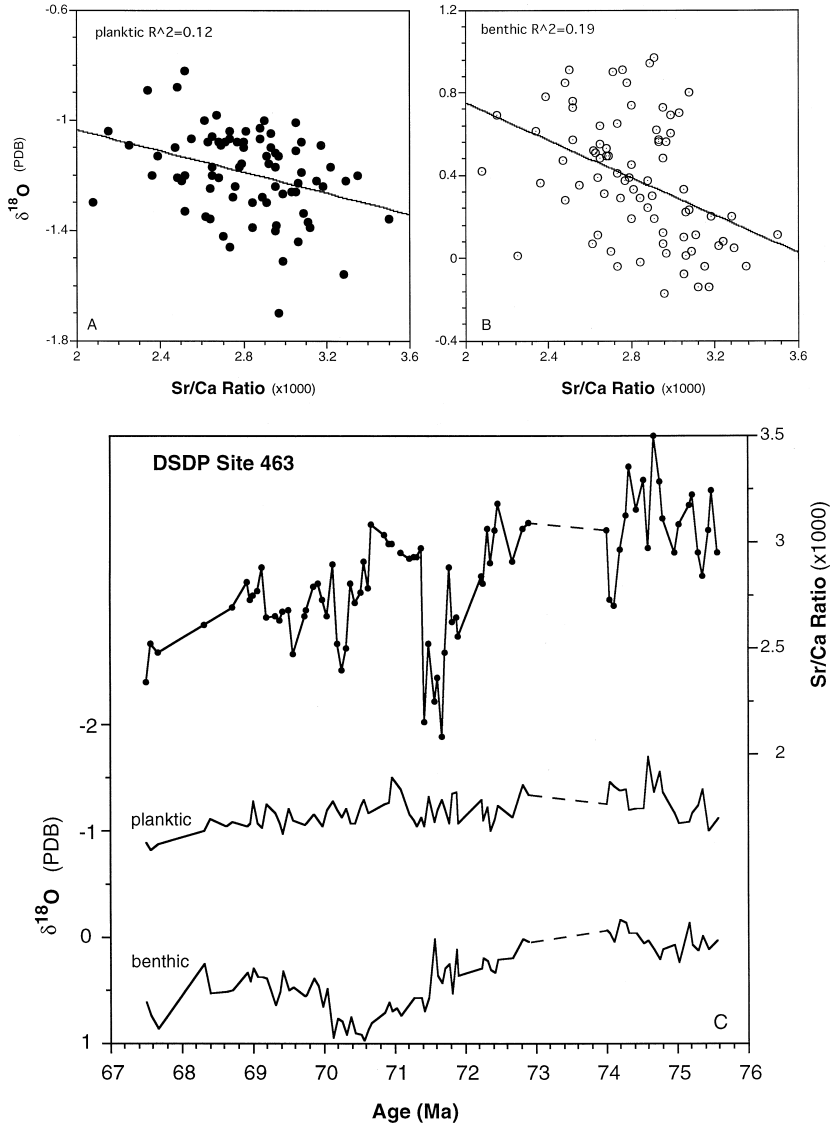

Fig. 2. a, b. Plots of benthic and planktic $\delta^{18}O$ vs. Sr/Ca ratios at Site 463. Note that the correlation coefficient is very low ($R^2 = 0.12$ for planktic foraminifera and $R^2 = 0.19$ for benthic foraminifera). This suggests diagenetic effects may not have significantly altered the isotopic values. c. Time series plot of benthic and planktic $\delta^{18}O$ values and the Sr/Ca ratio at Site 463. Note that the trend in benthic $\delta^{18}O$ values mirrors the trends observed in middle and high latitude Sites 525, 690 and 689 and suggest that there is no significant diagenetic overprint. The Sr/Ca ratio trends also show patterns which are consistent with climatic and sea level fluctuations and hence also suggest that diagenetic effects may be insignificant at Site 463.

base of Zone CF6 (Fig. 3; Li and Keller, 1998a). In contrast, Bralower et al. (1995) proposed that this boundary be placed at the base of C30N, which corresponds to within the middle of Zone CF4 (*R. fructicosa* Zone) at about 67.6 Ma (Fig. 3). In this study we tentatively use the first appearance of *R. fructicosa* to approximate the early-late Maastrichtian boundary at 68.3 Ma based on biostratigraphic correlation with the geomagnetic time scale at DSDP Site 525 (Li et al., 1999).

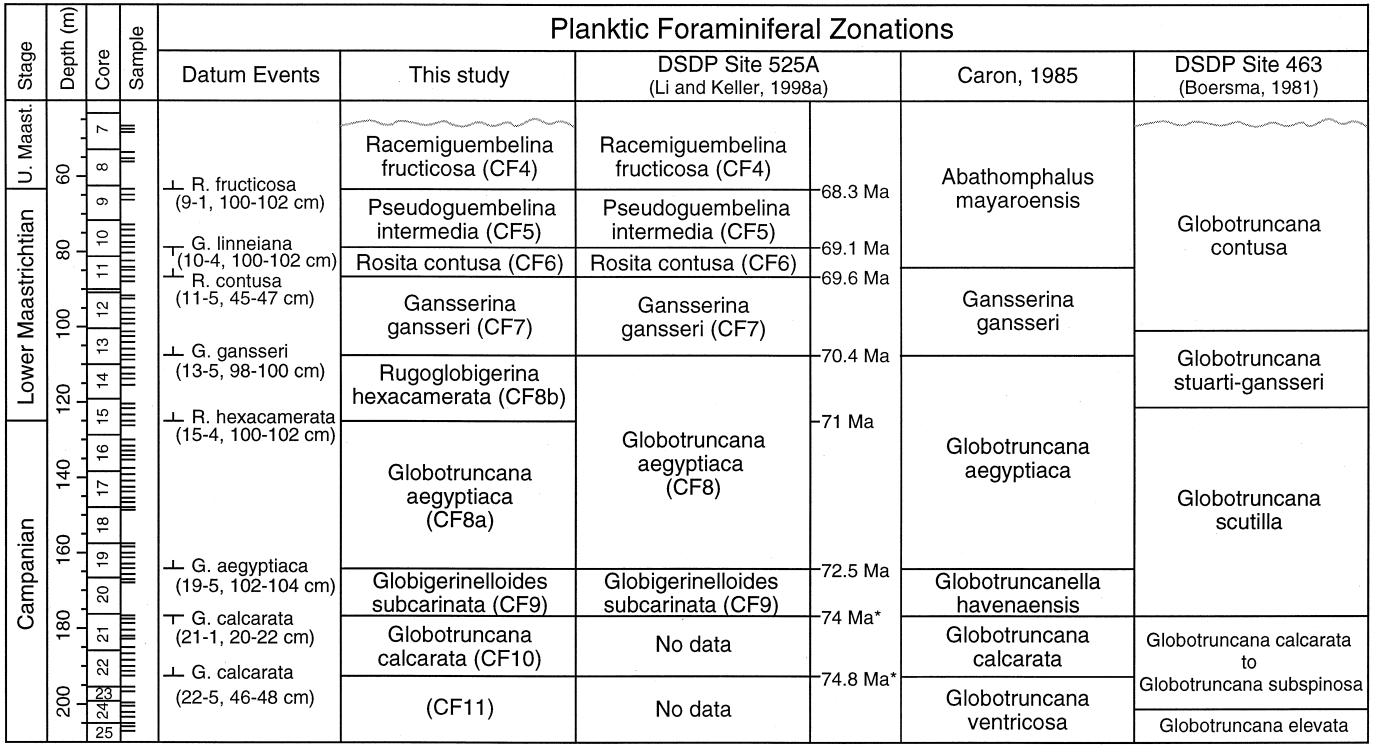

Fig. 3. Planktic foraminiferal biozonations and estimated ages for Site 463. Absolute ages were determined based on the revised time scale of Cande and Kent (1995), the paleomagnetic records of DSDP Sites 525 and 690, and the correlation of planktic foraminiferal datum events between these sites and DSDP Sites 463. Note that Site 463 has a major hiatus that spans the late Maastrichtian and early Danian from 67.5–64.5 Ma.

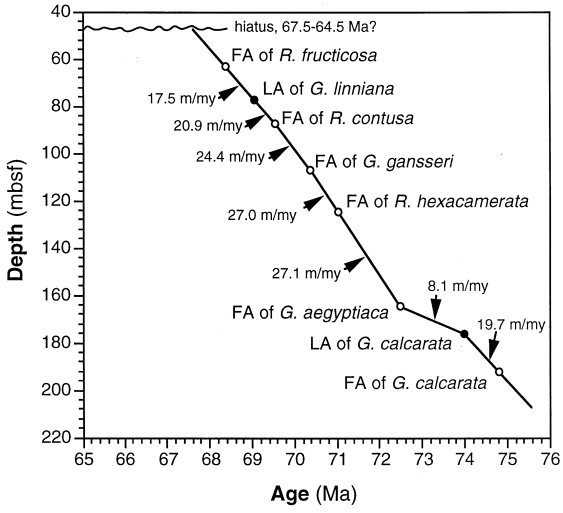

Fig. 4. Depth vs. age plot for Site 463. See Fig. 3 for calculation of absolute ages for datum events. Note that the relatively constant sedimentation rates suggest continuous deposition from 75 Ma to 67.5 Ma. However, low sedimentation rates between 74 Ma and 72.5 Ma suggest a hiatus or condensed interval.

3.3. Age model

We have calculated absolute ages for biozones based on the magnetostratigraphy of Sites 525 (Chave, 1984) and 690 (Hamilton, 1990) and the revised time scale of Cande and Kent (1995). In the absence of magnetostratigraphy at Site 463, absolute age estimates for this section were determined based on correlation of planktic foraminiferal datum events with Site 525. The linear depth vs. age plot for Site 463 (Fig. 4) based on this correlation suggests that there is little diachroneity of datum events between these two localities. This observation is independently supported by the similar stable isotope stratigraphy between Sites 463 and 525. This suggests that correlation errors between these sites may be relatively insignificant.

4. Results

4.1. Stable isotopes: site 463

In the late Campanian between 75.5–74 Ma, benthic (*Nuttalides truempyi*) $\delta^{18}O$ values averaged 0.05‰ (Zones CF11–CF10), but gradually increased by 1‰ between 74–70.4 Ma and reached maximum values of 0.97‰ between 70.6–70.1 Ma (CF8–CF7 transition, Fig. 5). At about 70 Ma, $\delta^{18}O$ values rapidly decreased 0.5‰ and remained lighter until ~68.4 Ma, followed by a sharp increase of 0.6‰ between 68.2 Ma and 67.8 Ma (Zones CF7–4). In contrast, surface (*Rugoglobigerina rugosa*) $\delta^{18}O$ values narrowly fluctuate between −1.01‰ and −1.70‰ during the late Campanian (75.6 to 71 Ma), and between −1‰ and −1.25‰ between 71 Ma and 68.5 Ma (Fig. 5).

The $\delta^{13}C$ record at Site 463 also shows strong trends. Between 75.6 Ma and 71 Ma benthic $\delta^{13}C$ values generally varied from 0.5‰ to 1.0‰ (Fig. 5). Minimum $\delta^{13}C$ values of 0.3‰ preceded maximum benthic $\delta^{18}O$ values of about 1‰ between 70.6 Ma and 70.1 Ma (CF8–7). Between 70.1 Ma and 68.5 Ma, benthic $\delta^{13}C$ gradually increased from 0.3‰ to a maximum of 1.28‰ (top of CF5). At about 68 Ma (CF4) benthic $\delta^{13}C$ decreased by 0.6‰ corresponding with a short-term rapid increase in benthic $\delta^{18}O$ values (Fig. 5).

Planktic $\delta^{13}C$ trends differ significantly. Between 75.6 Ma and 73 Ma planktic $\delta^{13}C$ values increased from 2.2‰ to 3.0‰ (CF11–CF9, Fig. 5). Thereafter, $\delta^{13}C$ values suddenly dropped 0.8‰ (CF9) coincident with a 0.4‰ increase in $\delta^{18}O$ values near the onset of the long-term gradual $\delta^{18}O$ decrease between 74 Ma and 70.4 Ma. Between this drop in $\delta^{13}C$ and 70.6 Ma, $\delta^{13}C$ values fluctuated between 2.2‰ and 2.5‰. Thereafter and coincident with the onset of the long-term increase in benthic $\delta^{13}C$ and maximum $\delta^{18}O$ values, planktic $\delta^{13}C$ increased by 0.6‰ near the top of CF8 followed by high $\delta^{13}C$ values (2.7‰) between 70.4 Ma and 69.6 Ma (CF7, Fig. 3). Subsequently planktic $\delta^{13}C$ values gradually decreased to 2‰ between 69 and 68 Ma.

4.2. Paleotemperatures

Between 75.6 Ma and 74 Ma intermediate water temperatures (IWT) in the equatorial Pacific Site 463 were relatively stable and ranged between 9.7°C and 11.5°C. Thereafter (date uncertain because of missing core at Site 463), IWT cooled gradually and reached maximum low temperatures of 6.5°C between 70.6 Ma and 70.1 Ma.

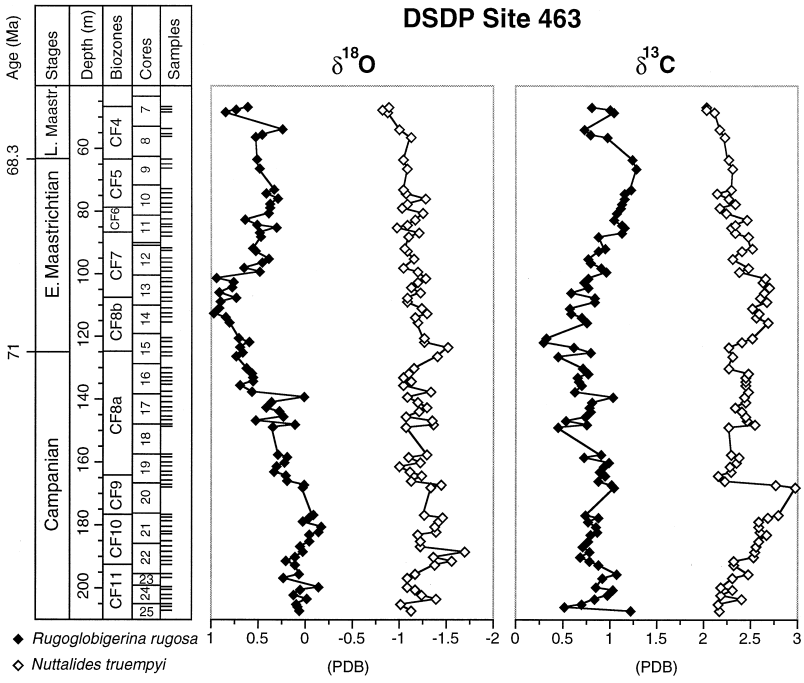

Fig. 5. Stable isotopes at the equatorial Pacific DSDP Site 463. Note that benthic foraminiferal $\delta^{18}O$ values increased gradually during the late Campanian and lowermost Maastrichtian and reached maximum values between 71–70 Ma (CF8–CF7 transition).

Significantly different IWT changes are observed in this time interval in the middle latitude South Atlantic Site 525 where IWT suggests a stepwise cooling (Fig. 6). At about 73 Ma paleotemperatures averaged 13.8°C and are followed by a rapid cooling to 10.4°C by 72.5 Ma and to 8.9°C by 71.6 Ma. IWT remained cool until 70.2 Ma. At the southern high latitude Site 690, IWT changes are similar to Site 525, though 0.5°C to 1°C cooler (Fig. 6). These paleotemperature records indicate that IWT in the equatorial Pacific was 2–3°C cooler during the 70.6–70.1 Ma maximum global cool event than in middle or high latitude South Atlantic.

After the maximum cool event, between 70.1 Ma and 69.9 Ma, IWT rapidly increased from 6.5°C to 9°C in the equatorial Pacific (Site 463) and from 9°C to 11.9°C in the middle latitude South Atlantic (Site 525), but remained cool in the high latitudes (Site 690, Fig. 6). Between 69.9 Ma and 68.2 Ma IWT remained warm in both the equatorial Pacific and middle latitude South Atlantic, whereas in the southern high latitudes IWT remained cool. At about 68 Ma IWT cooled from 9.7°C to 7°C in the equatorial Pacific, from 13.2°C to 9.8°C in the middle latitude Atlantic and from 8.4°C to 7°C in the high latitude South Atlantic. Between 67.5 Ma and 66.5 Ma, paleotemperatures averaged 9.2°C and 7°C in middle and high southern latitudes, respectively. No data are available for the equatorial Pacific for this interval. A major climatic event between 65.4 Ma and 65 Ma resulted in a rapid increase in IWT by 3–4°C globally, followed by rapid cooling of 2–3°C during the last 200 ka of the Maastrichtian (Stott and Kennett, 1990; Li and Keller, 1998a,c; Fig. 6).

Sea surface temperatures (SST) are characterized by greater fluctuations in middle latitudes than in low and high latitudes during the late Cretaceous, though this is partly due to differences in sample density between the sites (see also Barrera and Huber, 1990; Stott and Kennett, 1990; Li and Keller, 1998a,c; Fig. 6). Between 75.6 Ma and 74 Ma, tropical SST varied from 17.1°C to 20.2°C, comparable to the paleo-SST of 17–20°C estimated from the eastern equatorial Pacific (Boersma and Shackleton, 1981). Between 73 and 70.4 Ma, SST varied from 17°C to 19.3°C in the equatorial Pacific at a time

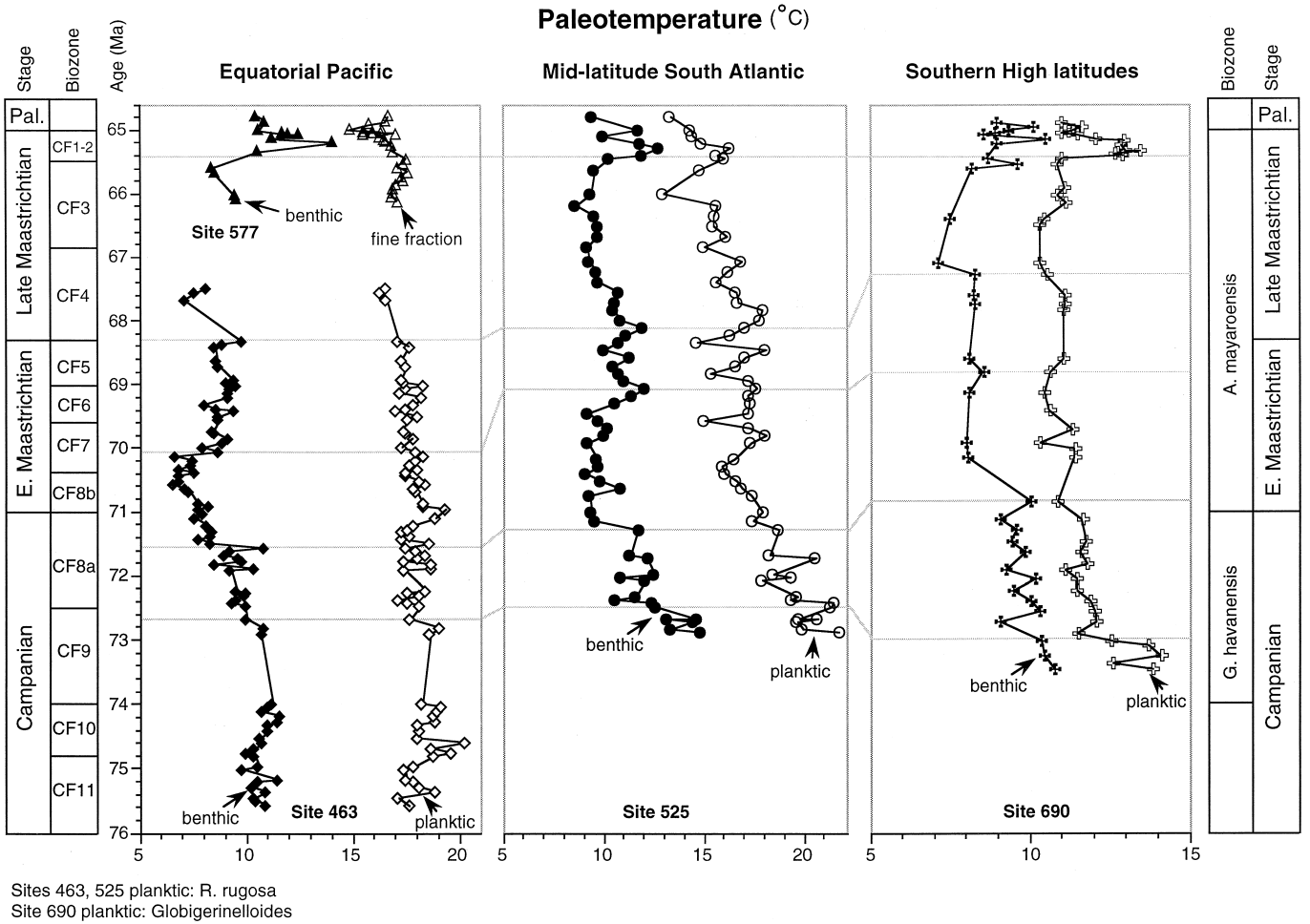

Fig. 6. Late Cretaceous paleotemperatures for the equatorial Pacific and middle and high latitude South Atlantic. Low and middle latitude IWT decreased 5–6°C at 73–70 Ma and reached maximum low temperatures between 71–70 Ma. SST decreased significantly in the middle and high latitudes, but remained relatively stable in the tropics. Near the end of the Cretaceous, a short-term warming terminated the long-term cooling trend and was followed by rapid cooling during the last 200 ka of the Maastrichtian. Planktic species: *Rugoglobigerina rugosa* at Site 463 and 525 and *Globigerinelloides* at Site 690. Benthic species: *Nuttalides truempyi* at Sites 463 and 690 and *Anomalinoides acuta* at Site 525. Biozones for Sites 463 (this study) and 525 from Li and Keller (1998a) and Barrera and Huber (1990) for Site 690.

when IWT cooled by 5°C. In contrast, SST decreased gradually from 15.8°C to 21.6°C between 72.8 Ma and 70.4 Ma in the middle latitude South Atlantic. But in the southern high latitudes, SST decreased 2.5°C at 73 Ma and remained relatively constant at ~11.5°C between 72.9 Ma and 71 Ma.

During the warm interval between 70.4 Ma and 68 Ma SST trends are more similar globally. In the equatorial Pacific and middle latitude South Atlantic SST averaged between 17°C and 18°C, whereas in southern high latitudes SST averaged 10.5°C. Between 68 Ma and 66.2 Ma SST gradually decreased from 17.6°C to 14.9°C and dropped to 12.8°C by 66 Ma. Insufficient data are available for this interval from the equatorial Pacific due to a hiatus at Site 463.

The major climatic event between 65.4 Ma and 65 Ma is also expressed in SST globally. At 65.5 Ma cool temperatures are recorded in intermediate waters globally and in surface waters of middle and high latitudes (Fig. 6). This cooling is followed by rapid warming of 3°C and 2.5°C in middle and high latitude SST and 3–4°C in IWT, though available data for SST in the tropics (Site 577) show little change. During the last 200 ka of the Maastrichtian both SST and IWT decreased by 2–3°C globally (Fig. 6; see also Zachos et al., 1989; Stott and Kennett, 1990; Li and Keller, 1998a,c).

4.3. Latitudinal thermal gradients

We calculated average SST and IWT in 5 time slices, which were chosen to span periods of relatively stable IWT (Fig. 7, Table 3). This simplified illustration of latitudinal thermal gradients illustrates the marked differences in IWT and similarities in SST.

SST latitudinal thermal gradient trends are generally as expected with tropical SST the warmest and high latitude SST the coolest. The one exception occurs in the 73–72.5 Ma interval (T1) where the SST in the middle latitude South Atlantic averaged

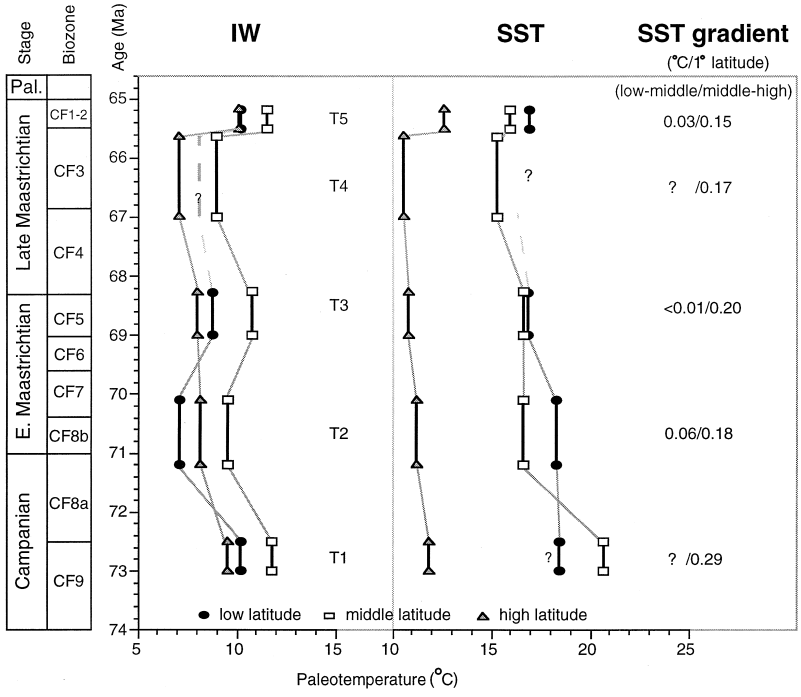

Fig. 7. Intermediate (IWT) and sea surface temperatures (SST) averaged for five time intervals for the tropical Pacific and middle and high latitude South Atlantic. Note that IWT are higher in middle latitudes than in low and high latitudes except for T5. SST decreased significantly in middle latitudes from T1 to T2, and gradually between other time intervals except for T5, when SST increased globally. Latitudinal SST gradients are low, suggesting high heat transport and an expanded tropical–subtropical zone.

Table 3
Paleotemperatures (degree) estimated for five time intervals during the late Cretaceous

	T5 (65.2–65.5 Ma)		T4 (65.6–67 Ma)		T3 (68.3–69 Ma)		T2 (70.1–71.1 Ma)		T1 (72.5–73 Ma)	
	Surface	Deep	Surface	Deep	Surface	Deep	Surface	Deep	Surface	Deep
Site 463					16.8	8.9	18.3	7.1	18.3	10.2
Site 525	15.9	11.6	15.2	9.0	16.6	10.9	16.5	9.6	20.4	11.9
Site 689					10.4	8.0	10.6	8.0	10.4	9.1
Site 690	12.6	10.1	10.2	7.2	10.9	8.1	11.2	8.9	11.9	9.8

19.5°C, as compared to an average of 18.3°C at the equatorial Site 463. This inverse temperature relationship may be an artifact of small sample numbers and the higher temperature variability at Site 525 (19–22°C), as compared with Site 463 (17.5–19°C, Fig. 6), though diagenetic effects cannot be excluded. Similarly, the average SST between 69 Ma and 68 Ma in tropical and middle latitudes reflect high SST variations at Site 525 ranging from 14.8°C to 17.8°C (Fig. 6). Alternatively, the relatively low equatorial Pacific SST, relative to the middle latitudes, may reflect increased evaporation during these relatively warm intervals. As evaporation increases, salinity fluctuates between 34–36‰ in the modern eastern equatorial Pacific (Broecker, 1989) and salinity may differ regionally depending on precipitation and evaporation patterns. Modeling simulations suggest an increase of 10% in evaporation during the Maastrichtian (Bush and Philander, 1997). Salinity fluctuations may thus partly account for the variability in calculated SST between middle and low latitudes.

In the modern oceans the SST latitudinal gradient averages 0.20°C/1° latitude for the low-middle latitude and 0.62°C/1° latitude for the middle-high latitude (Sverdrup et al., 1942). In contrast, the estimated latitudinal SST gradients for the Maastrichtian are significantly lower and for warm climatic intervals (T1, T3 and T5) range from 0.01–0.06°C/1° latitude between low and middle latitudes and between 0.15–0.29°C/1° latitude between middle and high latitudes. During cooler intervals (T2 and T4), the latitudinal SST gradients are 0.03°C/1° latitude between low and middle latitudes and 0.17–0.18°C/1° latitude between middle and high latitudes. These gradients are comparable to the 0.21°C/1° latitude gradient estimated by Barron (1983), but 1/3 lower than the 0.3°C/1° latitude gradient estimated by Wolfe and Upchurch (1987) from North American terrestrial vegetation. The very weak low to middle latitude SST gradients during both warm and cool climatic intervals suggest an expanded tropical–subtropical zone into middle latitudes, as also supported by the very similar planktic foraminiferal assemblages between the Tethys ocean and middle latitudes (Li and Keller, 1998a,b).

IWT are highly variable. Temperatures in the southern high latitudes are consistently 1–1.5°C cooler than in the equatorial Pacific with two exceptions. (1) Between 71–70 Ma, equatorial Pacific IWT are 2–3°C cooler than southern high latitude IWT; and (2) between 65.4 and 65.2 Ma, equatorial Pacific IWT are about the same as in southern high latitudes (Fig. 7). For the maximum cooling between 67.5 and 66 Ma equatorial temperatures are not well constrained due to widespread erosion and hiatuses which accompanied this global cooling and sea-level lowstand. Nevertheless, available data from Site 577 indicate very cool intermediate waters (Fig. 7).

IWT for the middle latitude Site 525 are consistently 2–3°C warmer than equatorial Pacific IWT (Fig. 7). One explanation for the higher temperatures is the possibly somewhat shallower paleodepth of Site 525 during the late Campanian and Maastrichtian, though available paleodepth data seem to be in conflict. The subsidence curve of Moore et al. (1984), which is based on a simple thermal cooling rate, shows a paleodepth of about 250 m at 70 Ma and possibly reaching 1000 m by K/T boundary time. However, paleodepth estimates based on benthic faunas and trace fossils suggest a deeper slope environment. For example, in the same study Moore et al. (1984 p. 885) cite a slope paleodepth estimate for the Late Campanian *G. tricarinata* Zone (correlates to our Late Campanian Zones CF8 and CF9) and paleodepths ranging between 1000 m to 1500 m

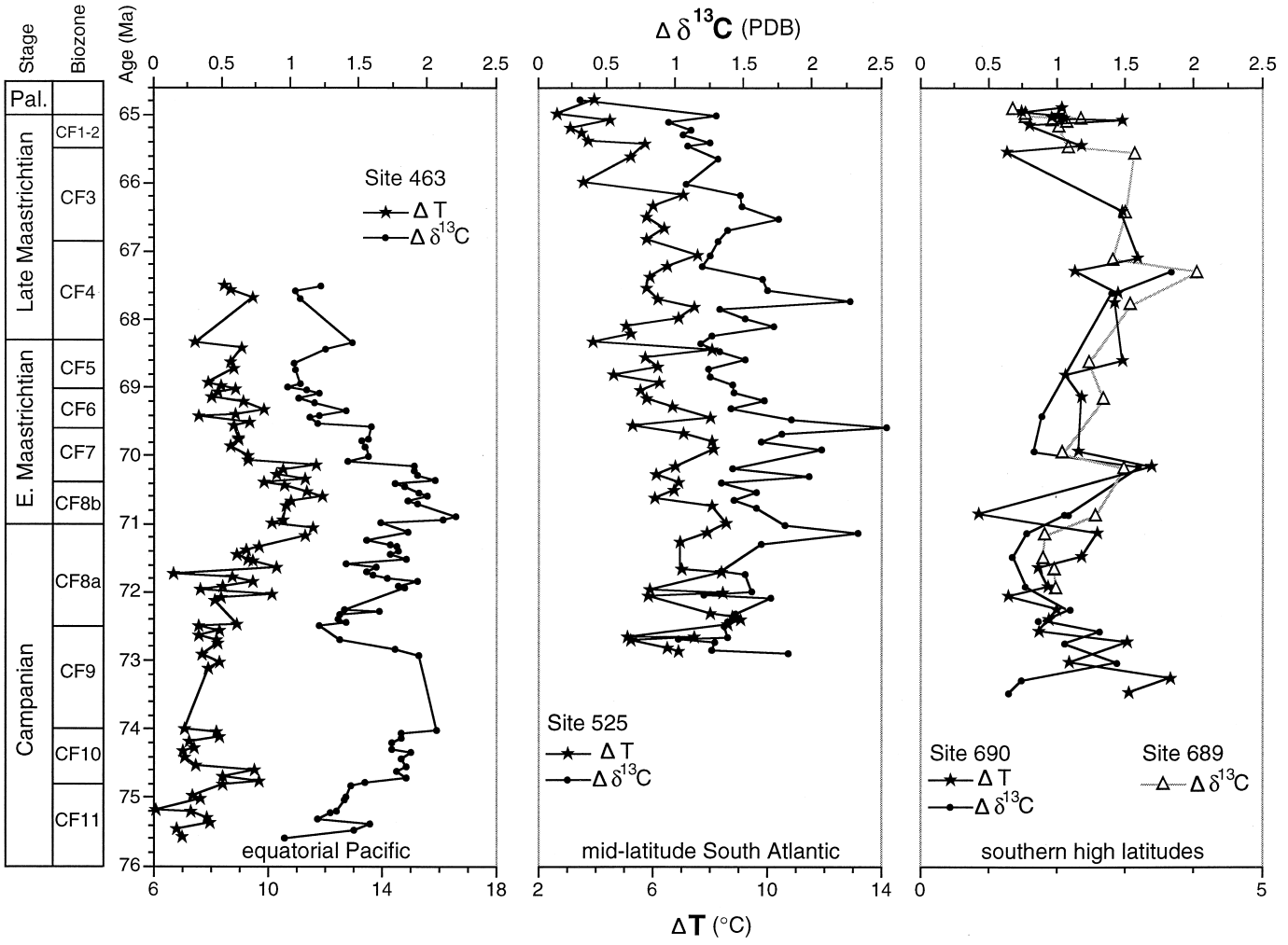

Fig. 8. Late Cretaceous vertical thermal and $\delta^{13}C$ gradients in low, middle and high latitudes. Covariance in ΔT and $\Delta\delta^{13}C$ suggests that surface productivity is a major controlling factor for late Cretaceous climate changes.

during the Late Campanian to Maastrichtian. In another paper by Fütterer (1984 p. 547), the paleodepth is estimated as between 1000–2000 m in the Maastrichtian based on *Halo* burrows which prefer deeper environments. More recently, D'Hondt and Arthur (1996) and Frank and Arthur (1999) estimated the paleodepth of Site 525 at about 1200 m (within intermediate waters) and more in keeping with the biotic data.

4.4. Vertical $\delta^{13}C$ and thermal gradients

Photosynthesis preferentially removes $^{12}CO_2$ leaving surface waters enriched in $^{13}CO_2$. As a result, surface dwelling planktic foraminifera have higher $\delta^{13}C$ than benthic foraminifera and bottom waters contain more ^{12}C due to oxidation of the sinking organic matter from surface waters. Thus, variations in surface productivity can be evaluated by the changes in surface-to-deep $\delta^{13}C$ gradients ($\Delta\delta^{13}C$) (Broecker and Peng, 1982). Changes in climate and ocean circulation can be evaluated by $\Delta\delta^{13}C$ and the surface-to-deep thermal gradient (ΔT). During the late Campanian and Maastrichtian both ΔT and $\Delta\delta^{13}C$ generally show similar trends (Fig. 8). Though late Cretaceous oceans are characterized by very low ΔT as compared to those in the modern ocean.

Between 75.6 Ma and 73 Ma in the equatorial Pacific, ΔT fluctuated between 6°C and 9.7°C. At the same interval $\Delta\delta^{13}C$ values gradually increased from 1‰ to 2‰, suggesting increased surface productivity. At 73 Ma, $\Delta\delta^{13}C$ rapidly decreased 0.7‰, whereas ΔT remained between 7 and 8°C. Fig. 5 shows that at this time benthic $\delta^{13}C$ decreased and planktic values remained relatively unchanged. This suggests that the $\Delta\delta^{13}C$ gradient change may reflect a change in deep ocean circulation and organic carbon accumulation derived from biological pumping at some other region of the ocean. Between 72.5 Ma and 68.5 Ma ΔT and $\Delta\delta^{13}C$ covaried. Vertical thermal gradients increased from 7.7°C at 72.5 Ma to a maximum of 11.7°C between 70.6 Ma and 70.1 Ma. At the same time $\Delta\delta^{13}C$ values increased by 1.1‰ and reached a maximum of 2–2.3‰ between 71 Ma and 70.1 Ma (Fig. 8). This indicates that climatic cooling was accompanied by increased surface productivity. At 70 Ma ΔT dropped from 11.7°C to 8.7°C and $\Delta\delta^{13}C$ dropped from 2‰ to 1.5‰, suggesting both climate warming and decreased surface productivity. Between 70 Ma and 68.5 Ma $\Delta\delta^{13}C$ decreased further from 1.5‰ to 1.0‰, whereas ΔT ranged between 7.9°C and 9.1°C. No tropical record is available for the later Maastrichtian (67.5–65 Ma).

In the high latitude South Atlantic Ocean (Site 690) ΔT and $\Delta\delta^{13}C$ trends are similar to the tropical Pacific, though lower sample resolution makes detailed comparisons impossible. Overall, however, ΔT varied from a low of 1°C to a high of 3.5°C, whereas $\Delta\delta^{13}C$ ranged from 0.75‰ to 1.5‰, with the exception of a single point increase to 2‰ in Site 689 at about 68.4 Ma.

In the middle latitude South Atlantic both ΔT and $\Delta\delta^{13}C$ are significantly more variable than in either the tropical Pacific or the high latitude South Atlantic (Fig. 8). During the global cooling between 73 Ma and 70 Ma, ΔT varied from 5.1°C to 8.6°C and $\Delta\delta^{13}C$ increased by 1‰. During the subsequent global warming between 70 Ma and 68.3 Ma, ΔT decreased to 3.9°C and $\Delta\delta^{13}C$ decreased by an average of 0.75‰. Between 68 Ma and 66.5 Ma, ΔT varied from 5°C to 7.6°C and decreased to 3.5°C during the global warming at the end of the Cretaceous. During the same interval $\Delta\delta^{13}C$ gradually decreased an average of 0.5‰ by 65.2 Ma and dropped 1‰ across the K–T boundary.

5. Discussion

The $\delta^{18}O$ and $\delta^{13}C$ records from the equatorial Pacific (Site 463), middle latitude South Atlantic (Site 525) and southern high latitudes (Site 690) show dramatic climatic changes during the late Cretaceous (Fig. 7). Climatic trends indicate global cooling of intermediate and surface waters, except for tropical SST, by 3–5°C beginning at 73 Ma and reaching maximum cool temperatures between 70.6 Ma and 70.1 Ma. At 70.1–70 Ma IWT increased by 2°C in the tropics and 4°C in the middle latitude South Atlantic and remained warm until 68.5 Ma, though IWT remained relatively unchanged during this time in the southern high latitudes. Between 68.5

Ma and 65.5 Ma IWT cooled by 2.5°C and SST cooled by 2°C and 1°C. Insufficient data are available for this interval in the tropics to estimate paleotemperatures. At 65.4 Ma intermediate and surface waters warmed rapidly by 4°C and 3°C, respectively, in the high latitude South Atlantic and by 3°C and 1°C respectively, in the middle latitude South Atlantic. In the tropical Pacific, IWT also warmed and reached temperatures equal to the middle latitude South Atlantic, whereas SST remained relatively unchanged. During the last 100–200 ka of the Cretaceous, IWT and SST cooled globally.

Climatic forcing has been linked to variations in atmospheric CO_2 due to volcanic degassing in the Cretaceous (Barron and Washington, 1982; Arthur et al., 1985; Frakes, 1986). Variations in pCO_2 generally result from carbon transfer from one reservoir to the other in the ocean–atmosphere and biomass–land ecosystems. The climatic variations during the late Cretaceous may have resulted from complex interaction among two or more forcing factors (e.g., changes in pCO_2, heat transport and paleogeographic configuration). The mechanisms include cooling from increased albedo, increased fertility (greening of oceans), increased carbon transfer from biomass on land to seawaters, increased land exposure or mountain build-up due to sea-level regressions and tectonic activity leading to reorganization of ocean circulation patterns (Frank and Arthur, 1999).

Changes in surface productivity ($\Delta\delta^{13}C$) provide an index for carbon transfer between atmosphere and ocean. During the global cooling between 70.5–72.5 Ma, the global increase in $\Delta\delta^{13}C$ suggests a decrease in pCO_2 (Fig. 8). Enhanced organic carbon influx from continents to oceans may have occurred during this time of global cooling and low sea levels. Because organic matter $\delta^{13}C$ values are much more negative ($-21‰$ to $-25‰$) than mean $\delta^{13}C$ values (0.0‰) in seawater, this would result in decreased $\delta^{13}C$ values. Between 70–68 Ma, $\Delta\delta^{13}C$ decreased during global warming and continued to decrease during the subsequent global cooling between 68–65.5 Ma (at Site 525, Fig. 8). The continued $\Delta\delta^{13}C$ decrease during the late Maastrichtian cooling suggests increased carbon transfer from atmosphere to the ocean and hence decreased pCO_2. The short-term (200–300 ka) global warming near the end of the Cretaceous is related to a major decrease in surface productivity, as indicated by decreased $\Delta\delta^{13}C$ values, which may have resulted from increased pCO_2 and may have coincided with major Deccan Trap volcanic degassing (Courtillot et al., 1988, 1996; Baksi, 1994).

The redistribution of heat on Earth's surface is an important component of the global heat balance (Frakes, 1979; Barron, 1983; Barron et al., 1993). The tropical zone receives a surplus of incoming solar radiation as compared with the polar areas. Nearly two-thirds of the excess heat gained in low latitudes is transported from the tropics poleward by the atmosphere and the remaining one-third by surface currents in the oceans (Nieuwolt, 1977; Riehl, 1979; Hastenrath, 1985). During the late Cretaceous, the latitudinal SST thermal gradients calculated for the 5-time intervals show no significant changes between warm and cool periods (Fig. 7), which suggests that high heat transport prevailed from equator to poles.

Warm polar regions and low latitudinal thermal gradients are most likely related to variations in the sources and modes of deep water circulation (e.g., Kennett and Stott, 1991). During warm climates, high latitude deep water sources may be reduced and/or replaced by warm saline deep water produced by evaporation in low to middle latitude areas (Brass et al., 1982; Kennett and Stott, 1990, 1991). GCM studies suggest deep water source areas may be highly sensitive to changes in paleogeographic configurations (Barron and Peterson, 1991), such as may be caused by local tectonics movements or global sea-level regressions, which may result in restricted deep water flow patterns. During the last 9 Ma of the Cretaceous, major eustatic regressions lowered sea-level by an estimated 70 m between 71 Ma and 70 Ma and 100 m between 68 Ma and 67 Ma (Haq et al., 1987) and additional sea-level fluctuations have recently been identified from the southwestern Tethys ocean (Li et al., 1999, Li et al., in press; Fig. 9). These major sea-level regressions significantly changed the paleogeographic configurations of the ocean topography at times of sea-level lows and highs and may have resulted in major changes in deep water circulation. During times of major cooling and sea-level regressions deep water sources may have been significantly reduced or shutdown in low to middle latitudes due to decreased

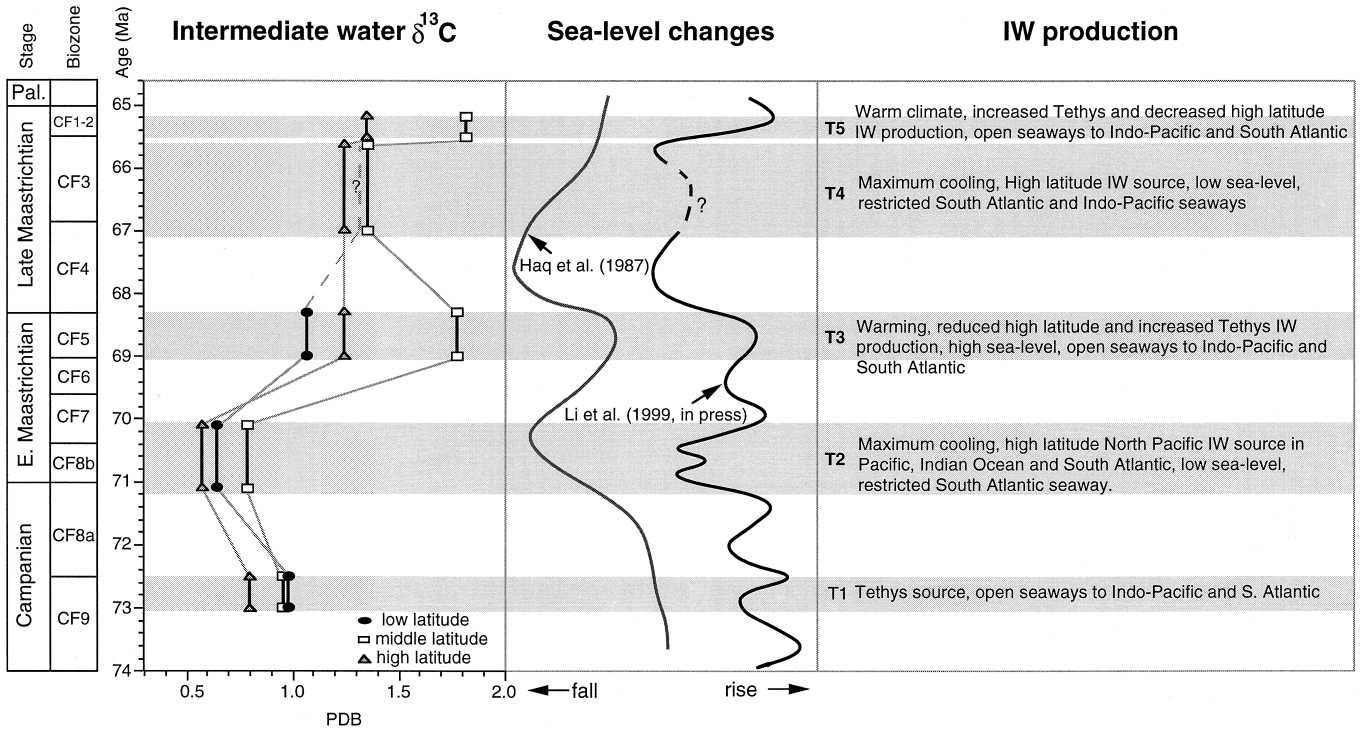

Fig. 9. Averaged intermediate water (IW) $\delta^{13}C$ values for five time intervals. Note that averaged IW $\delta^{13}C$ values are significantly heavier in the middle latitudes as compared with low and high latitude values during the warm intervals, except for T1. This suggests that the middle latitude South Atlantic was closer to the production of warm saline intermediate waters.

shallow continental seas and/or closure of seaways. In contrast, during times of significantly warmer high latitude temperatures than today, the production of deep water may have occurred by different processes and in different locations which produced complex patterns of deep and intermediate water circulation, oceanic turnover and nutrients cycling in the Maastrichtian oceans as shown by the simplified benthic $\delta^{13}C$ patterns for the five time slices (Fig. 9).

For example, during the cool climates between 70–71 Ma (T2) and 65.5–67 Ma (T4, Fig. 9), stable isotope data indicate a major decrease in IW $\delta^{13}C$ values in the middle latitude South Atlantic that suggests significantly reduced deep water production in low latitudes, coupled with low sea-levels and restricted seaways. In addition, the equatorial Pacific received a short-term influx of cool waters from the high latitude North Pacific (Dickens and Owen, 1995; Barrera et al., 1997), as suggested by IWT that are cooler than in the southern high latitudes and heavier benthic $\delta^{13}C$ values. Frank and Arthur (1999) suggest that the east–west tectonic features of the Walvis Ridge and Rio Grande Rise in the South Atlantic may have effectively blocked the northward flow of deep and intermediate waters at this time. However, they also conclude that during the early Maastrichtian cooling (70–71 Ma) deep waters formed at high latitudes in both the North Atlantic and North Pacific. Though North Atlantic deep water production may have occurred at this time, our data suggest that the North Pacific source predominated in the equatorial Pacific, Indo-Pacific and South Atlantic (see also Barrera et al., 1997; Dickens and Owen, 1995).

During times of warm climates between 68–69 Ma (T3) and again between 65.2–65.4 Ma (T5, Fig. 9), average intermediate water (IW) $\delta^{13}C$ values are higher in the middle latitude South Atlantic than in the southern high latitudes and the equatorial Pacific, or equal in the tropics and middle latitudes as observed during the late Campanian (T1, Fig. 9). This suggests that at these times the middle latitude South Atlantic was closest to the source of IW production and implies that the low latitude Tethys may have been the likely source, especially for T5 (Li and Keller, 1998c). During these warm climates and generally high sea-levels, IW production in the shallow Tethys region may have significantly increased and seaways were probably open to the South Atlantic and the Indo-Pacific. Though, Frank and Arthur (1999) do not believe that warm saline bottom water production in the low latitude Tethys played an important role during the Maastrichtian climate warmings, their compilation of published data does not include the high resolution dataset from the last two million years of Site 525 which strongly suggests enhanced heat transport from the tropics (Li and Keller, 1998c).

6. Summary

Stable isotope analyses of late Cretaceous benthic and planktic foraminifera from the tropical Pacific Site 463, middle latitude Site 525 and high latitude South Atlantic Sites 689 and 690 indicate major changes in climate and alternating low and high latitude sources of intermediate water formation. These data suggest the following observations.

1. Between 73 and 70 Ma intermediate water temperature (IWT) decreased by 5–6°C globally and SST by 4–5°C in the middle and high latitudes. Intermediate waters warmed by 2°C at 70–68.5 Ma in low and middle latitudes. Global cooling resumed between 68.5–65.5 Ma and IWT decreased by 3–4°C and SST by 3°C in middle latitudes.

2. Rapid global warming increased IWT and SST by 3–4°C at between about 450–200 ka before the K–T boundary. During the last 200 ka of the Cretaceous, climate cooled rapidly with a 2–3°C decrease in both IWT and SST.

3. During the global climate warming between 65.2–65.4 Ma, the middle latitude South Atlantic was closest to the source of IW production and implies that the low latitude Tethys played a major role in global climate change.

4. During the global cooling at 71–70 Ma and possibly at 67–65.5 Ma, the sources of cold intermediate waters in the equatorial Pacific, Indo-Pacific and South Atlantic were derived from the high latitude North Pacific.

5. Climate changes, sea-level fluctuations and associated restricted seaways appear to be the most likely mechanisms for the alternating sources of IW production.

Acknowledgements

We would like to thank the reviewers William Ruddiman and Michael Arthur for their comments and suggestions for improvement, the Ocean Drilling Program for providing samples for this study, Dan Bryan for measuring stable isotopes for DSDP Site 463, and Lowell Stott for providing stable isotopic data of benthic foraminifera from ODP Sites 689 and 690. This study was supported by NSF OCE 9021338.

References

Abreu, V.S., Hardenbol, J., Haddad, G., Baum, G.R., Droxler, A.W., Vail, P.R., 1998. Sequence stratigraphy of the European basins. Society of Economic Paleontologists and Mineralogists Spec. Publ. 60, 75–80.

Arthur, M.A., Dean, W.E., Schlanger, S.O., 1985. Variations in the global carbon cycle during the Cretaceous related to climate, volcanism, and changes in atmospheric CO_2. In: Sunquist, E.T., Broecker, W.S. (Eds.), The Carbon Cycle and Atmospheric CO_2: Natural Variations Archean to Present. Geophysical Monograph, 32: 504–529.

Baker, P.A., Gieshes, J.M., Elderfield, H., 1982. Diagenesis of carbonates in deep-sea sediments-evidence from Sr/Ca ratios and interstitial dissolved Sr^{2+} data. Journal of Sedimentology and Petrology 52, 71–82.

Barrera, E., 1994. Global environmental changes preceding the Cretaceous–Tertiary boundary: early-late Maastrichtian transition. Geology 22, 877–880.

Barrera, E., Huber, B.T., 1990. Evolution of Antarctic waters during the Maestrichian: Foraminifera oxygen and carbon isotope ratios, Leg 113. In: Barker, P.F., Kennett, J.P., et al. (Eds.), Proceeding of the Ocean Drilling Program, Scientific Results, 113: 813–827.

Barrera, E., Huber, B.T., Savin, S.M., Webb, P.N., 1987. Antarctic marine temperatures: late Campanian through Early Paleocene. Paleoceanography 2, 21–47.

Barrera, E., Savin, S.M., Thomas, E., Jones, C.E., 1997. Evidence for thermohaline-circulation reversals controlled by sea-level change in the latest Cretaceous. Geology 25, 715–718.

Barron, E.J., 1983. A warm equable Cretaceous: the nature of the problem. Earth-Science Review 19, 305–338.

Barron, E.J., Peterson, W.H., 1991. The Cenozoic ocean circulation based on ocean General Circulation Model results. Palaeogeography Palaeoclimatology Palaeoecology 83, 1–28.

Barron, E.J., Washington, W.M., 1982. Warm Cretaceous climates, high atmospheric CO_2 as a pausible mechanism. In: Sunquist, E.T., Broecker, W.S. (Eds.), The Carbon Cycle and Atmospheric CO_2: Natural Variations Archean to Present, Geophysical Monograph, 32: 546–553.

Barron, E.J., Peterson, W.H., Pollard, D., Thompson, S.L., 1993. Past climate and the role of ocean heat transport: model simulation for the Cretaceous. Paleoceanography 8, 785–798.

Baksi, A.K., 1994. Geochronological studies on whole-rock basalts, Deccan Traps, India: evaluation of the timing of volcanism relative to the K–T boundary. Earth and Planetary Science Letters 121, 43–56.

Boersma, A., 1981. Cretaceous and early Tertiary foraminifers from Deep Sea Drilling Project Leg 62 Sites in the central Pacific. In: Thiede, J., Vallier, T.L., et al. (Eds.), Initial Reports of Deep Sea Drilling Project, 62: 377–397.

Boersma, A., Shackleton, N.J., 1981. Oxygen- and carbon-isotope variation and planktonic-foraminifera depth habitats, late Cretaceous to Paleocene, Central Pacific, Deep Sea Drilling Project sites 463 and 465. In: Thiede, J., T.L. Vallier, et al. (Eds.), Initial Reports of Deep Sea Drilling Project, 62: 513–526.

Bralower, T.J., Leckie, R.M., Sliter, W.V., Thierstein, H.R., 1995. An integrated Cretaceous microfossil biostratigraphy. In: Berggren, W.A, Kent, D.V., Aubry, M.P., Hardenbol, J. (Eds.), Geochronology, Time Scale and Global Stratigraphic Correlation, Society of Economic Paleontologists and Mineralogists, 54: 65–79.

Brass, G.W., Southam, J.R., Peterson, W.H., 1982. Warm saline bottom water in the ancient ocean. Nature 296, 620–623.

Broecker, W.S., 1989. The salinity contrast between the Atlantic and Pacific oceans during glacial time. Paleoceanography 4, 207–212.

Broecker, W.S., Peng, T.-H., 1982. Tracers in the Sea. Eldigio, Palisades.

Bush, A.B.G., Philander, S.G., 1997. The late Cretaceous: simulation with a coupled atmosphere–ocean general circulation model. Paleoceanography 112, 495–516.

Cande, S.C., Kent, D.V., 1995. Revised calibration of the geomagnetic polarity timescale for the Late Cretaceous and Cenozoic. Journal of Geophysical Research 100, 6093–6095.

Caron, M., 1985. Cretaceous planktic foraminifera. In: Bolli, H.M., Saunders, J.B., Perch-Nielsen, K. (Eds.), Plankton Stratigraphy, Cambridge Univ. Press, Cambridge, p. 17–86.

Chave, A.D., 1984. Lower Paleocene-Upper Cretaceous magnetostratigraphy, Sites 525, 527, 528, and 529, Deep Sea Drilling Project Leg 74. In: Moore, T.C., Jr., Rabinowitz, P.D., et al. (Eds.), Initial Reports of Deep Sea Drilling Project, 74: 525–531.

Courtillot, V., Feraud, G., Maluski, H., Vandamme, D., Moreau, M.G., Besse, J., 1988. Deccan flood basalts and the Cretaceous/Tertiary boundary. Nature 333, 843–846.

Courtillot, V., Jaeger, J.J., Yang, Z., Feraud, G., Hofmann, C., 1996. The influence of continental flood basalts on mass extinctions; where do we stand? In: Ryder, G., Fastovosky, D., Gartner, S. (Eds.), The Cretaceous–Tertiary Event and other Catastrophes in Earth history, Geological Society of America, Special Paper, 307: 513–525.

D'Hondt, S., Arthur, M.A., 1996. Late Cretaceous oceans and the cool tropic paradox. Science 271, 1838–1841.

D'Hondt, S., Lindinger, M., 1994. A stable isotopic record of the

Maastrichtian ocean–climate system: South Atlantic DSDP Site 528. Palaeogeography Palaeoclimatology Palaeoecology 112, 363–378.

Dickens, G.R., Owen, R.M., 1995. Chinook through rifting and hydrothermal deposition at Sites 885 and 886. In: Barker, P.F., Kennett, J.P., et al. (Eds), Proceeding of the Ocean Drilling Program, Scientific Results, 145: 413–426.

Douglas, R.G., Savin, S.M., 1973. Oxygen and carbon isotope analysis of Cretaceous and Tertiary foraminifera from the central North Pacific. Initial Reports of Deep Sea Drilling Project 17, 591–605.

Douglas, R.G., Savin, S.M., 1975. Oxygen and carbon isotope analysis of Cretaceous and Tertiary foraminifera from Shatsky Rise and other sites in the North Pacific Ocean. Initial Reports of Deep Sea Drilling Project 32, 509–520.

Erez, J., Luz, B., 1983. Experimental paleotemperature equation for planktonic foraminifera. Geochimica et Cosmochimica Acta 47, 1025–1031.

Frakes, L.A. Climates Throughout Geological Time. Elsevier, New York, 1979.

Frakes, L.A., 1986. Mesozoic-Cenozoic climate history and causes of the glaciation. In: Hsu, K.J. (Ed.), Mesozoic and Cenozoic oceans. Geodynamics Series, 15: 33–48.

Frank, D.T., Arthur, M.A., 1999. Tectonic forcings of Maastrichtian ocean-climate evolution. Paleoceanography 14, 103–117.

Fütterer, D.K., 1984. Bioturbation and trace fossils in deep sea sediments of the Walvis Ridge, Southeastern Atlantic, Leg 74. In: Moore, T.C., Jr., Rabinowitz, P.D., et al. (Eds.), Initial Reports of Deep Sea Drilling Project, 74: 543–555.

Gradstein, F.M., Agterberg, F.P., Ogg, J.G., Hardenbol, J., Van Veen, P., Thierry, J., Huang, Z., 1994. A Mesozoic time scale. Journal of Geophysical Research 99, 24051–24074.

Hamilton, N., 1990. Mesozoic magnetostratigraphy of Maud Rise, Antarctica. In: Barker, P.F., Kennett, J.P., et al. (Eds.), Proceeding of the Ocean Drilling Program, Scientific Results, 113: 255–260.

Haq, B.U., Hardenbol, J., Vail, P.R., 1987. Chronology of fluctuating sea levels since the Triassic. Science 235, 1156–1167.

Hastenrath, S., 1985. Climate and Circulation of the Tropics. Reidel, Boston, 455 pp.

Huber, B.T., 1990. Maestrichtian planktonic foraminifer biostratigraphy of the Maud Rise (Weddell Sea, Antarctica): ODP Leg 113 holes 689 and 690C. Proceedings of the Ocean Drilling Program, Scientific Results 113, 489–513.

Huber, B.T., Hodell, D.A., Hamilton, C.P., 1995. Middle-late Cretaceous climate of the southern high latitudes: stable isotopic evidence for minimal equator-to-pole thermal gradients. Bulletin of Geological Society of America 107, 1164–1191.

Keller, G., 1989. Extended Cretaceous–Tertiary boundary extinctions and delayed population changes in planktonic foraminifera from Brazos River, Texas. Paleoceanography 4, 287–332.

Kennett, J.P., Stott, L.D., 1990. Proteus and Proto-Oceanus, Paleogene Oceans as revealed from Antarctic stable isotopic results. In: Barker, P.F., Kennett, J.P., et al. (Eds.), Proceeding of the Ocean Drilling Program, Scientific Results, 113: 865–880.

Kennett, J.P., Stott, J.D., 1991. Abrupt deep-sea warming, paleoceanographic changes and benthic extinction at the end of Paleogene. Nature 353, 229–255.

Li, L., Keller, G., 1998a. Maastrichtian climate, productivity and faunal turnovers in planktic foraminifera in south Atlantic DSDP Site 525A and 21. Marine Micropaleontology 33, 55–86.

Li, L., Keller, G., 1998b. Diversification and extinction in Campanian–Maastrichtian planktic foraminifera of Northwestern Tunisia. Eclogae Geologicae Helvetiae 91, 75–102.

Li, L., Keller, G., 1998c. Abrupt deep-sea warming at the end of the Cretaceous. Geology 26, 995–998.

Li, L., Keller, G., Stinnesbeck, W., 1999. The Late Campanian and Maastrichtian in Northwestern Tunisia: palaeoenvironmental inferences from lithology, macrofauna and benthic foraminifera. Cretaceous Research 20, 231–252.

Li, L., Keller, G., Adatte, T., Stinnesbeck, W., in press. Late Cretaceous sea-level changes in Tunisia: a multi-disciplinary approach. Journal of Geological Society, London.

MacLeod, K.G., Huber, B.T., 1997. Reorganization of deep ocean circulation accompanying a late Cretaceous extinction event. Nature 380, 422–425.

Matthews, R.K., Poore, R.Z., 1980. Tertiary $\delta^{18}O$ record and glacio-eustatic sea-level fluctuations. Geology 8, 501–504.

Moore, T.C., Jr., Rabinnowitz, P.D., et al., 1984. Site 525. In: Moore, T.C., Jr., Rabinowitz, P.D., et al. (Eds.), Initial Reports of Deep Sea Drilling Project, 74: 873–894.

Nederbragt, A.J., 1991. Late Cretaceous biostratigraphy and development of Heterohelicidae (planktic foraminifera). Micropaleontology 37, 329–372.

Nieuwolt, S., 1977. Tropical Climatology: An introduction to the climates of the low latitudes. Wiley, New York, 207 pp.

Odin, G.S., 1996. Definition of a Global Boundary Stratotype Section and Point for the Campanian/Maastrichtian boundary. Bulletin de L'Institut Royal des Sciences Naturelles de Belgique, Sciences de La Terre 66, 111–117, Suppl.

Pardo, A., Ortiz, N., Keller, G., 1996. Latest Maastrichtian and Cretaceous–Tertiary boundary foraminiferal turnover and environmental changes at Agost, Spain. In: MacLeod, N., Keller, G. (Eds.), Cretaceous–Tertiary mass extinctions. W.W. Norton, p. 139–172.

Paull, C.K., Hills, S.J., Thierstein, H.R., 1988. Progressive dissolution of fine carbonate particles in pelagic sediments. Marine Geology 81, 27–40.

Richter, F.M., Liang, Y., 1993. The rate and consequences of Sr diagenesis in deep-sea carbonates. Earth and Planetary Science Letters 117, 553–565.

Riehl, H., 1979. Climates and Weather in the Tropics. Academic Press, London, 611 pp.

European Working Group on planktonic foraminifera, Robaszynski, F., Caron, M., Gonzalez Donoso, J.M., Wonders, A.A.H., 1983. Atlas of late Cretaceous Globotruncanids. Revue de Micropaleontologie 26 (3–4), 145–305.

Shackleton, N.J., Kennett, J.P., 1975. Paleotemperature history of

the Cenozoic and the initial of Antarctic glaciation: oxygen and carbon isotope analyses in DSDP Sites 277, 279, and 281. In: Kennett, J.P., Houtz, R.E., et al. (Eds.), Initial Reports of Deep Sea Drilling Project, 29: 743–755.

Shackleton, N.J., Hall, M.A., Boersma, A., 1984. Oxygen and carbon isotope data from Leg 74 foraminifers. Initial Reports of Deep Sea Drilling Project 74, 599–612.

Spero, H.J., 1992. Do planktic foraminifera accurately record shifts in the carbon isotopic composition of seawater ΣCO_2?. Marine Micropaleontology 19, 275–285.

Spero, H.J., Williams, D.F., 1988. Extracting environmental information from planktic foraminiferal $\delta^{13}C$ data. Nature 335, 717–719.

Spero, H.J., Lerche, I., Williams, D.F., 1991. Opening the carbon isotopic ''vital effect'' black box, 2, quantitative model for interpreting foraminiferal carbon isotope data. Paleoceanography 6, 639–655.

Spicer, R.A., Corfield, R.M., 1992. A review of terrestrial and marine climates in the Cretaceous with implications for modeling the ''Greenhouse'' Earth. Geological Magazine 129, 169–180.

Stott, L.D., Kennett, J.P., 1990. The paleoceanographic and paleoclimatic signature of the Cretaceous/Paleogene boundary in the Antarctic: Stable isotopic results from ODP Leg 113. In: Barker, P.F., Kennett, J.P., et al. (Eds.), Proceeding of the Ocean Drilling Program, Scientific Results, 113: 829–848.

Sverdrup, H.U., Johnson, M.W., Fleming, R.H., 1942. The Oceans. Prentice-Hall, Englewood Cliffs, NJ.

Thomas, E., 1990. Late Cretaceous through Neogene deep sea benthic foraminifera (Maude Rise, Weddell Sea, Antarctica). In: Barker, P.F., Kennett, J.P., et al. (Eds.), Proceeding of the Ocean Drilling Program, Scientific Results, 113: 571–594.

Wolfe, J.A., Upchurch, G.R., 1987. North American nonmarine climates and vegetation during the late Cretaceous. Palaeogeography Palaeoclimatology Palaeoecology 61, 33–77.

Wu, G., Berger, W.H., 1990. Planktic foraminifera: differential dissolution and the Quaternary stable isotope record in the west equatorial Pacific. Paleoceanography 4, 181–198.

Zachos, J.C., Arthur, M.A., Thunell, R.C., Williams, D.F., Tappa, E.J., 1985. Stable isotope and trace element geochemistry of carbonate sediments across the Cretaceous/Tertiary boundary at Deep Sea Drilling Project Hole 577 Leg 86. Initial Reports of Deep Sea Drilling Project 86, 513–532.

Zachos, J.C., Arthur, M.A., Dean, W.E., 1989. Geochemical evidence for suppression of pelagic marine productivity at the Cretaceous/Tertiary boundary. Nature 337, 61–64.